A Simple Analysis of the Effect of Construction Materials on Bridge Impact Factors

M.L. Peterson
Chin-Gwo Chiou
R. M. Gutkowski

Department of Civil Engineering
Colorado State University
Fort Collins, CO 80523

June 1999

ACKNOWLEDGEMENTS

The authors wish to extend their appreciation to Dr. Donald W. Radford for his guidance and supervision during the preparation of this report. Grateful acknowledgement also is given to Dr. Xiao Bin Le for his inspiring advice in this effort, to Colorado State University for the use of facilities and resources as well as cost sharing funds that were provided as a part of the MPC process and funding.

DISCLAIMER

TABLE OF CONTENTS

LIST OF TABLES

LIST OF FIGURES

EXECUTIVE SUMMARY

This research considers the influence of different construction materials on the dynamic impact factor of bridges. The general concept of the dynamic impact factor and typical evaluation methods are reviewed. A comparison of bridge codes from some countries is made. Then, a simply supported Euler-Bernoulli beam is used to evaluate influence of materials on the impact factor. A numerical example is shown with a constant vehicle loading substituted into the model using three different materials for the bridge system. Interesting results from the model suggest that the choice of construction material is a secondary factor in the dynamic impact factor. A large number of other factors can be evaluated in the same manner to determine which design parameters have the greatest influence on the dynamic impact factor. The simple method for evaluation of changes in the dynamic impact factor is expected to be useful to practitioners and students who are interested not only in the influence of material selection, but also on the other factors, such as pavement roughness.

1. INTRODUCTION

Overview

When a bridge receives vehicle loading, the vehicle suspension will react to roadway roughness by compression and extension of the suspension system. This oscillation creates wheel-axle forces that exceed the static weight during the time the acceleration is downward, and reduces the static weight when acceleration is upward. This phenomenon is referred to as “impact loading” or “dynamic loading,” commonly expressed as a portion of the static axle loads. The influence of dynamic loading on bridge loading usually is computed using the impact factor, also known as dynamic factor, or dynamic load allowance. The AASHTO specifications use the term impact factor, which also will be used in this report [1].

Impact factor is an important parameter in bridge design and evaluation. As the amount and weight of moving vehicles on roadways increase, the dynamic loading to a bridge system also increases, and in consequence, the impact factor becomes more important. Observations and measurements indicate that the dynamic behavior of a bridge system is a function of three primary factors [2]:

- dynamic properties of the vehicle (mass, suspension, axle configuration, tires, speed)
- road roughness (approach, roadway, cracks, potholes, waves)
- dynamic properties of the bridge structure (span, mass, support types, materials, geometry).

It has been well established that natural frequencies of a bridge system have the primary influence on its dynamic response. Material properties are an essential determinant of the natural frequencies of a bridge. The influence of material properties is a primary motivation for the research.

Many investigations have been made to evaluate the impact factor of bridges. Significantly less effort has been focused on the effect of construction materials on the impact factor. Hence, the intent of this paper is to focus on the influence of different materials on the impact factor. The outline of this paper is that a simple model based on a Lagrangian formulation of the Euler-Bernoulli beam is presented to

estimate the impact factor. This work is described after a review of definitions related to impact factor and a review of specifications related to bridge design codes. Finally, the accuracy of bridge design codes related to specifications of the impact factor will be examined using numerical data.

Definition of Impact Factor

The concept of a dynamic impact factor has been used in the design of bridges for years. Generally, it has been suggested that the impact factor is defined as the amount of force, expressed as a fraction of the static force, by which dynamic force exceeds static force. However, there is no uniformity in the manner by which this increment is calculated from test data. The different ways of calculating the dynamic increment can be easily explained using Figure 1.1, which is based on work by Bakht and Pinjarkar [3]. Data, such as shown in Figure 1.1, typically is constructed from actual field test data. Figure 1.1 shows the variation of the dynamic and static deflections at mid-span of a girder with respect to time. The dynamic deflections were obtained when the test vehicle traveled on the bridge at normal speed. Static deflections were obtained when the vehicle traveled at crawling speed so as not to induce dynamic magnification of deflections. Notation has been adopted for Figure 1.1 as follows:

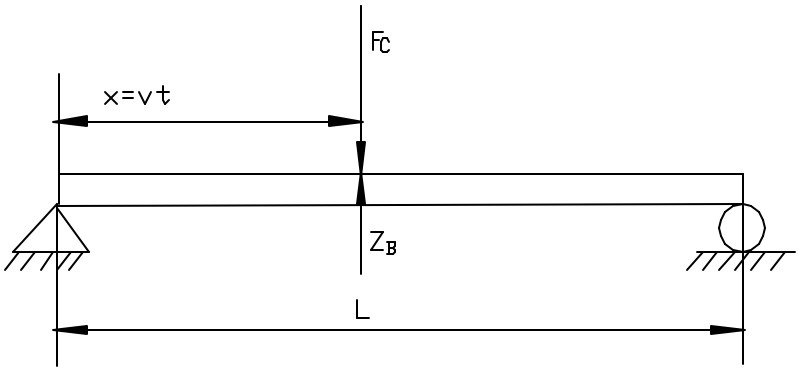

Figure 1.1: Mid-Span Deflections Under a Moving Vehicle Load.

d_{stat} = maximum deflection under the vehicle traveling at crawling speed.

d_{dyn} = maximum deflection under the vehicle traveling at normal speed. This deflection also denoted as $d_{\max}$.

d'_{stat} = maximum deflection obtained from the curve of median deflections. Note that d_{stat} and d'_{stat} do not necessarily take place at the same load location.

d_{min} = minimum dynamic deflection in the vibration cycle containing d_{max}.

d_1 = static deflection corresponding to d_{max}. d_1 is not necessarily the maximum static deflection.

d_2 = median deflection corresponding to d_{max}. (Median deflection is the mean deflection of dynamic peaks)

d_s^* = static deflection at the same location where Δ_1 is recorded.

Δ_1 = maximum difference between dynamic and static deflections; Δ_1 does not necessarily take place at the same load position that causes either d_{stat} or d_{dyn}.

Δ_2 = maximum difference between dynamic and median deflections.

Δ_3 = difference between dynamic and static deflections at the same load location that causes d_{stat}.

Δ_4 = difference between dynamic and median deflection at the same load location that causes d'_{stat}.

These various definitions have been used in the past to obtain the dynamic increment from test data. Depending on the application, similar parameters have been given different names. For the sake of convenience, all the parameters will be referred to as impact factors and denoted by the symbol IM. The following have been, at various times in the literature, used to describe dynamic effects on loading [3].

Definition 1

According to the definition of impact increment of dynamic response by Fuller et al. [4], the largest of IM would be given by:

$$IM = \Delta_1 / d_s^*$$

It should be noted, however, that this method is the result of a hypothetical and impractical extrapolation of a definition, which perhaps was not intended for this purpose.

Definition 2

A commonly used variation of Definition 1 is that IM taken as the ratio of the measured instantaneous dynamic response to the maximum static response. Thus,

$$\text{IM} = \Delta_3 / d_{stat}$$

This definition has been used in most analytical studies.

Definition 3

When the static deflections are assumed to be the same as median deflections, Definition 2 of IM changes to

$$\text{IM} = \Delta_4 / d'_{stat}$$

Definition 4

Definition 4 was used in Switzerland to interpret test data from the dynamic bridge tests conducted from 1949 to 1965 [5]. According to this definition, the dynamic increment IM is given by

$$\text{IM} = \frac{d_{\max} - d_{\min}}{d_{\max} + d_{\min}}$$

It is noted that this definition of the dynamic increment was abandoned in Switzerland after 1965 in favor of Definition 5.

Definition 5

According to the fifth definition, which has been used in Switzerland for tests conducted before 1945 and after 1965, the dynamic increment IM is given by

$$\text{IM} = \frac{d_{dyn} - d_2}{d_2}$$

Definition 6

A variation of Definition 5 would be when the static response corresponding to the maximum dynamic response is taken as the same as the median response obtained from the dynamic test data. In this case, IM is given by

$$\text{IM}=\frac{d_{dyn}-d_1}{d_1}$$

This definition has been extensively used to interpret results of many dynamic tests on bridges in Ontario [6].

Definition 7

In some research conducted in Ontario, applicability of the following expression was considered for obtaining IM [7]:

$$\text{IM}=\frac{d_{dyn}-d'_{stat}}{d'_{stat}}$$

Definition 8

If the actual static responses are used instead of median responses, the following variation of Definition 7 is obtained:

$$\text{IM}=\frac{d_{dyn}-d_{stat}}{d_{stat}}$$

Definition 9

A rational approach, proposed by B. Bakht and S. G. Pinjarkar, to compute a representative value of the impact factor from the test data is expressed by

$$\text{IM}=\frac{\bar{I}(1+c_v sb)}{a_L}$$

where

$\bar{I}$ = mean value of the dynamic amplification factor [3];

c_v = coefficient of variation of the dynamic amplification factor, that is , the ratio of standard deviation and mean;

s = the separation factor for dynamic loading, which has been found to have a value of 0.57 [3];

β = the safety index, from reliability based design, which typically has a value of about 3.5 for highway bridges; and

a_L = the live load factor

It is recommended that, in the absence of more rigorous analysis, the value of a_L should be taken as 1.4 [3], which also is the live load factor specified in the Ontario Code [8].

The broad range of definitions of IM based on measured responses is a consequence of the facts that, (a) the static response of a bridge is not necessarily the same as the median response obtained from the dynamic test data, and (b) the maximum static and dynamic responses do not always take place under the same load position. If the static and median responses were identical and the maximum static and dynamic responses took place simultaneously, the diversity of definitions of IM would disappear and Definitions 2 through 8 all would give the same value of IM for a given set of data [3].

International Perspective of Impact Factor

Figure 1.2 shows various bridge engineering design specifications from around the world, which use dramatically different factors [9]. The ordinate axis represents the load increase or impact factor and the abscissa is the fundamental frequency of the structure. The broad variation indicates that the international bridge design community has not yet reached a consensus about this issue. Figure 1.2 shows bridge design specifications before 1992, more recent design codes of some countries also are included in this paper since they have changed somewhat (AASHTO (USA) [1], OHBDC (Canada) [10], Highway bridge design code (Taiwan) [11], and Eurocode (European) [12]). The AASHTO bridge design code and OHBDC have been adopted by many countries. The Eurocode is accepted by most countries in the European community. A tendency is shown, among recent design codes, that specific numerical impact factors are used to replace formula based factors. For example, the previous AASHTO code [13] used an

impact formula that attempted to reflect dynamic behavior by using span length as a parameter. Another example, the Ontario Highway Design Bridge Code [4], modeled this behavior as a function of the natural frequency of the bridge system. But both the AASHTO and the OHBDC use specific numerical impact factors in the present design codes. Clearly, the present specification does not attempt to model dynamic effects with great accuracy, however the codes attempt to reflect, with sufficient accuracy and conservation, a reasonable factor needed for design. One of the objectives of this paper is to identify the reliability of the bridge design codes with respect to variation of the impact factor for different bridge construction materials. This comparison will be performed in the discussion following the numerical examples.

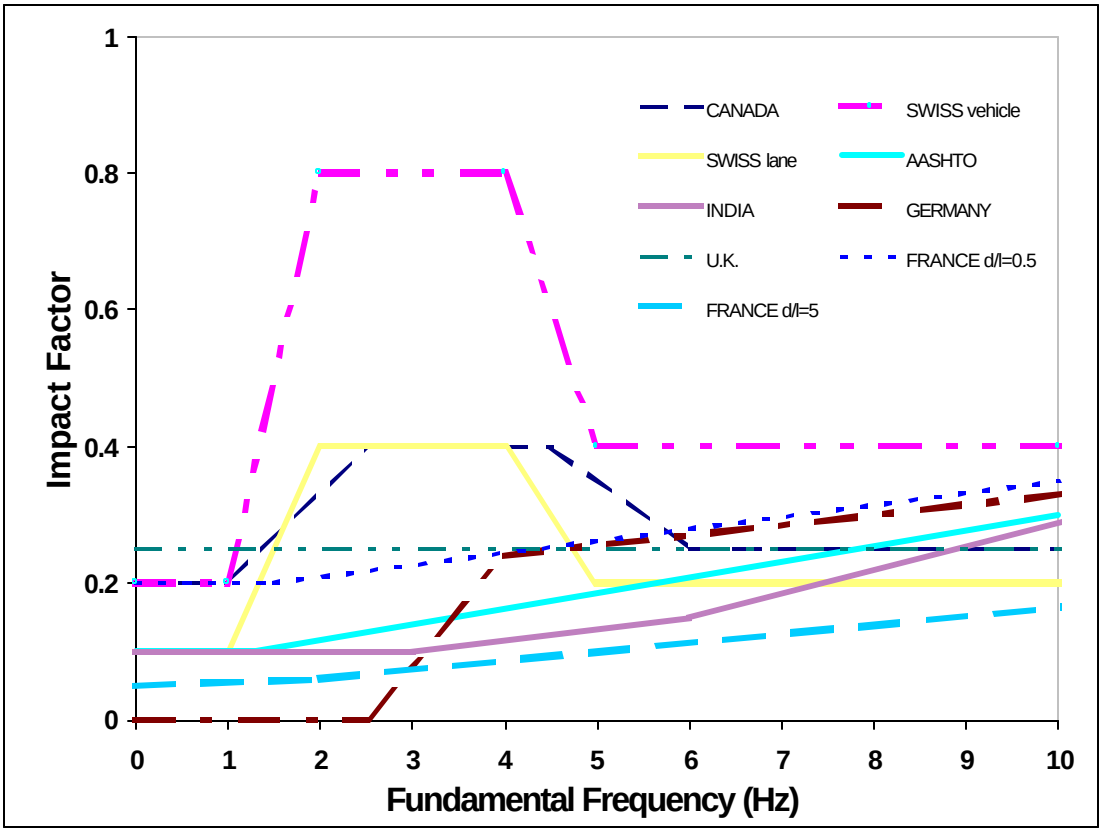

Figure 1.2: International Perspective of Impact Factor

2. THE SYSTEM MODEL AND EXAMPLES

Approach

The approach taken in this study was to develop a small analytical model that can be used to explore the sensitivity of bridge dynamic impact factors to a number of input variables. The initial model uses a simply-supported Euler-Bernoulli beam to approximate response of the bridge span. The outline of the approach is such that the derivations using the Lagrangian formulation of the Euler-Bernoulli (E-B) beam assumptions are appropriately reviewed first. Next, the model shape function of the system are found. Finally, the formula which determines deflection induced by a loading force at any location in the E-B beam is presented. After this development, numerical examples are generated. The purpose of this effort is to provide an overview of impact factors using a simple model system. This provides a foundation for which an improved model can be incorporated into subsequent phases of the study.

Review of Lagrangian Dynamics

Lagrange's equation, which is based upon energy concepts, is an extremely powerful device for analysis of dynamic systems. To develop this foundation and to make it match the assumptions associated with the Euler-Bernoulli beam, the configuration shown in Fig. 2.1, consisting of a simple beam supporting a group of j masses, M_r (r=1,2,…j), and subjected to a group of m forces, F_l (l=1,2,…m), is considered [14]. The deflected shape is defined by a set of N generalized coordinates,

q_i (I=1,2,…N).

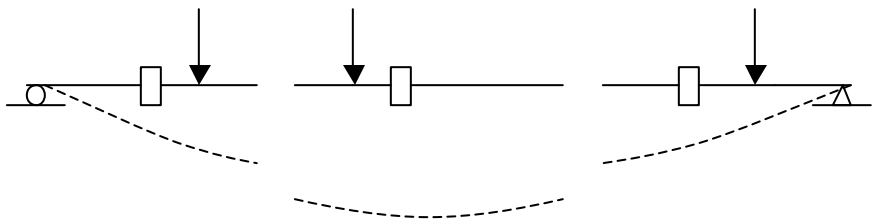

Figure 2.1: Lagrange's Equation ------ Notation

Suppose now that a virtual displacement is introduced consisting of a small change in one generalized coordinate, q_i. Let this change be designated by $d\,q_i$. By the principle of virtual work, the work done by external forces during the virtual disturbance must equal the corresponding change in internal strain energy. We may write the preceding statement as

$$d\,W_e + d\,W_{in} + d\,W_c = d\,U \tag{2.1}$$

where

$d\,W_e$ = virtual work done by external loads F_l

$d\,W_{in}$ = virtual work done by inertia forces

$d\,W_c$ = virtual work done by damping forces

$d\,U$ = change in internal strain energy

Three of these terms may be expressed simply as

$$d\,W_e = \frac{\partial W_e}{\partial q_i} d\,q_i \qquad \text{(a)}$$

$$d\,W_c = \frac{\partial W_c}{\partial q_i} d\,q_i \qquad \text{(b)} \tag{2.2}$$

$$d\,U = \frac{\partial U}{\partial q_i} d\,q_i \qquad \text{(c)}$$

and $d\,W_{in}$ may be expressed by

$$d\,W_{in} = -\sum_{r=1}^{j} (M_r y_r'') \frac{\partial y_r}{\partial q_i} d\,q_i$$

where y_r is the total displacement at mass r. $d\,W_{in}$ also can be expressed in the equivalent form as

$$d\,W_{in} = -\frac{d}{dt} \sum_{r=1}^{j} M_r y_r' \frac{\partial y_r}{\partial q_i} d\,q_i + \sum_{r=1}^{j} M_r y_r' \frac{\partial y_r'}{\partial q_i} d\,q_i \tag{2.3}$$

The equation shown in (2.3) is based upon the fact

$$\frac{d}{dt}(y_r' \frac{\partial y_r}{\partial q_i}) = y_r'' \frac{\partial y_r}{\partial q_i} + y_r' \frac{\partial y_r'}{\partial q_i}$$

Now, we define the kinetic energy K and its derivatives as

$$K = \sum_{r=1}^{j} \frac{1}{2} M_r y_r'^2 \qquad \text{(a)}$$

$$\frac{\partial K}{\partial q_i'} = \sum_{r=1}^{j} M_r y_r' \frac{\partial y_r'}{\partial q_i'} \qquad \text{(b)} \qquad (2.4)$$

$$\frac{\partial K}{\partial q_i} = \sum_{r=1}^{j} M_r y_r' \frac{\partial y_r'}{\partial q_i} \qquad \text{(c)}$$

Furthermore, since y_r is a function of q_i,

$$y_r' = \frac{\partial y_r}{\partial q_i} q_i' \text{ and } \frac{y_r'}{q_i'} = \frac{\partial y_r}{\partial q_i}$$

Equation (2.4b) may therefore, be rewritten as

$$\frac{\partial K}{\partial q_i'} = \sum_{r=1}^{j} M_r y_r' \frac{\partial y_r}{\partial q_i} \qquad (2.5)$$

If then Eqs. (2.4c) and (2.5) are substituted into Eq. (2.3), the result has the form

$$d W_{in} = -\frac{d}{dt}\left(\frac{\partial K}{\partial q_i'}\right) d q_i + \left(\frac{\partial K}{\partial q_i}\right) d q_i \qquad (2.6)$$

Finally, by substituting Eqs. (2.2) and (2.6) into Eq. (2.1) and canceling $d q_i$, equation (2.7) is obtained

$$\frac{d}{dt}\left(\frac{\partial K}{\partial q_i'}\right) - \frac{\partial K}{\partial q_i} + \frac{\partial U}{\partial q_i} - \frac{\partial W_c}{\partial q_i} = \frac{\partial W_e}{\partial q_i} \qquad (2.7)$$

Equation (2.7) shows the kinetic energy K, the strain energy U, the work done by the damping forces W_c, and the work done by real external forces W_e in terms of the generalized coordinates $q_1 \ldots q_N$. When these expressions are differentiated as indicated and substituted into Eq. (2.7), the result is an equation of motion. In the case under consideration, the term $\partial K / \partial q_i$ is zero, since kinetic energy is a function of velocity rather than of displacement. Hence, Lagrange's equation becomes

$$\frac{d}{dt}\left(\frac{\partial K}{\partial q_i'}\right)+\frac{\partial U}{\partial q_i}-\frac{\partial W_c}{\partial q_i}=\frac{\partial W_e}{\partial q_i} \tag{2.8}$$

Derivation of an Euler-Bernoulli (E-B) Beam

Assume a simply supported uniform beam with constant length (l), uniform distributed mass (m), mass per length (r), and flexural rigidity (EI) as shown in Fig. 2.2. From a free body of the beam and considering the influence of the kinetic energy, the equation of motion can be derived from Newton's second law. Note that small displacements will be assumed (ds=dx).

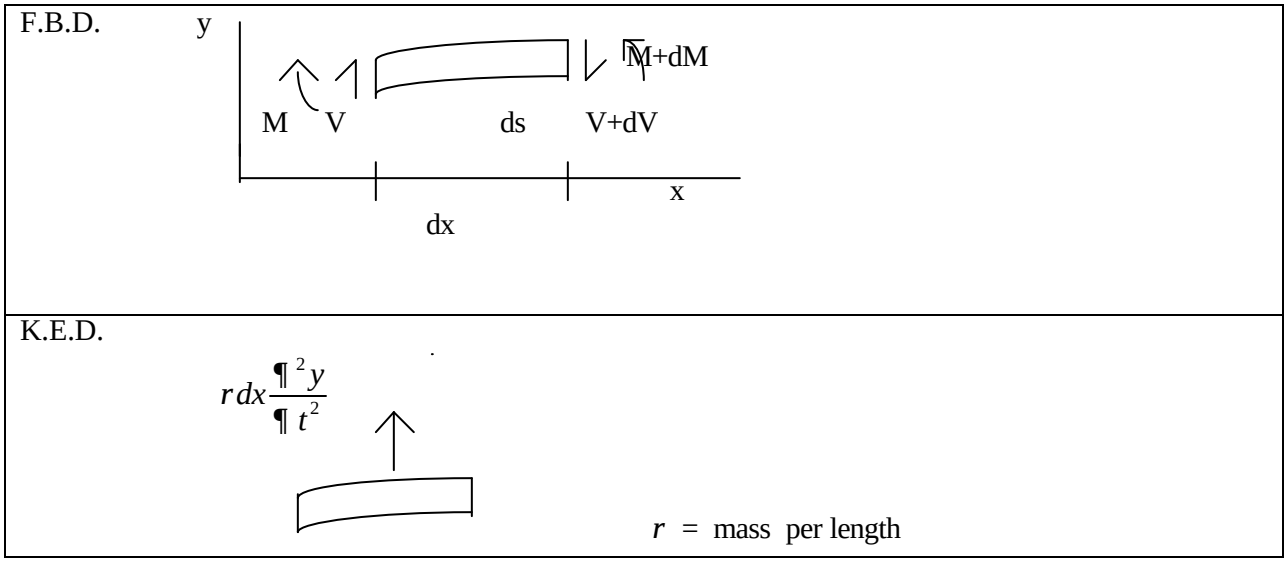

Figure 2.2: Free Body and Kinetic Energy Diagrams of a Simply Supported Beam

Adding forces in the vertical direction, Newton's second law implies that

$$\uparrow \sum F_y = Ma_y$$

From this addition it is then evident

$$[f(x,t)dx - dv] = r\,dx\frac{\partial^2 y}{\partial t^2}$$

The equation of motion could be expressed as

$$r\frac{\partial^2 y}{\partial t^2}+\frac{dv}{dx}=f(x,t) \tag{2.9}$$

The shear and moment of a beam are

$$v = \frac{dM}{dx}, M = EI\frac{d^2y}{dx^2}$$

which then produces from the second derivative

$$\frac{dv}{dx} = \frac{d^2}{dx^2}[EI\frac{\partial^2 y}{\partial x^2}] = EI\frac{\partial^4 y}{\partial x^4}$$

which is then substituted into (2.9), to arrive at

$$r\frac{\partial^2 y}{\partial t^2} + EI\frac{\partial^4 y}{\partial x^4} = f(x,t) \tag{2.10}$$

To get the normal model shape, we set f(x,t)=0 and use separation of variables. Assume

$$y(x,t) = X(x)T(t) \tag{2.11}$$

then substituted into (2.10) with f(x,t)=0, to arrive at

$$\frac{\P^2}{\P t^2}[X(x)T(t)] + (\frac{EI}{r})\frac{\P^4}{\P x^4}[X(x)T(t)] = 0$$

If set

$$(-\frac{EI}{r})\frac{X''''}{X} = \frac{T''}{T} = C \tag{2.12}$$

then the two domains of a Euler-Bernoulli beam are

$$(\frac{EI}{r})X'''' + CX = 0 \qquad \text{(mode shape)} \tag{2.13a}$$

$$T'' - CT = 0 \qquad \text{(time response)} \tag{2.13b}$$

To get the natural frequencies and the normal mode shapes of a E-B beam, we start with the equation (2.13a). Since C=+w^2 or C=0 gives no solution, we assume C=-w^2. Then

$$\Rightarrow X'''' - (\frac{w^2 r}{EI})X = 0$$

If, for this case,

$$\frac{w^2 r}{EI} = b^4$$

then, the resulting solution has the familiar form

$$X(x) = a\cosh(\beta x) + b\sinh(\beta x) + c\cos(\beta x) + d\sin(\beta x)$$

The second derivative of the equation is

$$X''(x) = a\beta^2\cosh(\beta x) + b\beta^2\sinh(\beta x) - c\beta^2\cos(\beta x) - d\beta^2\sin(\beta x)$$

Then it is necessary to impose boundary conditions as follows:

$$X(0) = 0 \Rightarrow a + c = 0$$

$$X(l) = 0 \Rightarrow a\cosh(\beta l) + b\sinh(\beta l) + c\cos(\beta l) + d\sin(\beta l) = 0$$

$$X''(0) = a - c = 0$$

$$X''(l) = a\beta^2\cosh(\beta l) + b\beta^2\sinh(\beta l) - c\beta^2\cos(\beta l) - d\beta^2\sin(\beta l) = 0$$

$$\Rightarrow a = c = 0$$

and

$$\begin{cases} b\sinh(\beta l) + d\sin(\beta l) = 0 \\ b\sinh(\beta l) - d\sin(\beta l) = 0 \end{cases}$$

$$\Rightarrow \begin{bmatrix} \sinh(\beta l) & \sin(\beta l) \\ \sinh(\beta l) & -\sin(\beta l) \end{bmatrix} \begin{Bmatrix} b \\ d \end{Bmatrix} = 0$$

For a non-zero solution, the determinant of the matrix of the coefficients must equal zero. Then, it is necessary to

$$\begin{vmatrix} \sinh(\beta l) & \sin(\beta l) \\ \sinh(\beta l) & -\sin(\beta l) \end{vmatrix} = 0$$

which has the result

$$\Rightarrow -2\sinh(\beta l)\sin(\beta l) = 0$$

since $\sinh(\beta l) \neq 0$ if $\beta l \neq 0$

$$\Rightarrow \sin(\beta l) = 0 \text{, and b=0}$$

$$\Rightarrow \beta_n l = np,\ \beta_n = \frac{np}{l},\ n = 1,2,3,....$$

$$\Rightarrow \frac{w_n{}^2 r}{EI} = b_n{}^4, w_n = b_n{}^2\sqrt{\frac{EI}{r}} = (\frac{np}{l})^2\sqrt{\frac{EI}{r}}, n = 1,2,3,....$$

The solution for the shape function is then

$$X_n(x) = \sin(b_n x) = \sin(\frac{npx}{l}) \qquad (2.14)$$

This gives the familiar shape functions associated with the E-B beam.

The System Model

To determine the response of an E-B beam due to applied forces, the Lagrange's equation will be used.

From Eq. (2.11)

$$y(x,t) = \sum_{n=1}^{\infty} X_n(x)T_n(t)$$

The velocity of the beam is then given by

$$y'(x,t) = \sum_{n=1}^{\infty} X_n(x)T_n'(t)$$

The kinetic energy of the complete system can be expressed as

$$K = \frac{1}{2} r \int_0^l y'^2 dx = \frac{1}{2} r \int_0^l [\sum_{n=1}^{\infty} X_n(x)T_n'(t)]^2 dx$$

Expanding the series, we arrive at

$$K = \frac{1}{2} r \int_0^l [\sum_{n=1}^{\infty} X_n^2(x)T_n'^2(t)]dx + r\int_0^l \{\sum_{n=1}^{\infty}[X_n(x)T_n'(t)][X_m(x)T_m'(t)]\}dx$$

The second term indicates the sum of all the modal cross products, which is equal to zero because of the orthogonal condition of the shape function. Then

$$K = \frac{1}{2} r \int_0^l [\sum_{n=1}^{\infty} X_n^2(x)T_n'^2(t)]dx = \frac{1}{2} r \sum_{n=1}^{\infty} T_n'^2 \int_0^l X_n^2(x)dx$$

and

$$\frac{\partial K}{\partial T_n'} = rT_n' \int_0^l X_n^2(x)dx$$

$$\frac{d}{dt}\frac{\partial K}{\partial T_n'} = rT_n'' \int_0^l X_n^2(x)dx$$

The work done by external forces during an arbitrary distortion is

$$W_e = \int_0^l f(x,t)[\sum_{n=1}^{\infty} X_n(x)T_n(t)]dx = \int_0^l F(t)p(x)[\sum_{n=1}^{\infty} X_n(x)T_n(t)]dx$$, if we set f(x,t)=F(t)p(x)

The rate of change of external work with respect to T_n is therefore

$$\frac{\partial W_e}{\partial T_n} = F(t)\int_0^l p(x)X_n(x)dx$$

The internal strain energy is

$$U = \int_0^l \frac{M^2}{2EI}dx = \int_0^l \frac{1}{2EI}(EI\frac{d^2y}{dx^2})^2 dx = \frac{EI}{2}\int_0^l (\sum_{n=1}^{\infty} T_n X_n'')^2 dx$$

The rate of change of internal strain energy with respect to T_n is therefore

$$\frac{\partial U}{\partial T_n} = EIT_n \int_0^l (X_n'')^2 dx$$

$$\because X_n = \sin(\frac{np}{l}x), \therefore (X_n'')^2 = (\frac{np}{l})^4 (X_n)^2$$

Then

$$\frac{\partial U}{\partial T_n} = EI(\frac{np}{l})^4 T_n \int_0^l (X_n)^2 dx$$

Writing the Lagrange's equation (2.8) with damping omitted and substituting from the above, we obtain

$$\frac{d}{dt}\frac{\partial K}{\partial T_n'} + \frac{\partial U}{\partial T_n} = \frac{\partial W_e}{\partial T_n}$$

$$rT_n'' \int_0^l X_n^2(x)dx + EI(\frac{np}{l})^4 T_n \int_0^l X_n^2 dx = F(t)\int_0^l p(x)X_n(x)dx \qquad (2.15)$$

Since we know by previous definition (Eq. (2.12)) that, if the last equation (2.15) is divided by the coefficient of T_n'', the coefficient of T_n becomes w_n^2. Thus

$$T_n''(t) + w_n^2 T_n(t) = \frac{F(t)\int_0^l p(x)X_n(x)dx}{r\int_0^l X_n^2(x)dx} \tag{2.16}$$

If damping is then added, equation (2.16) then becomes

$$T_n''(t) + 2x_n w_n T_n'(t) + w_n^2 T_n(t) = \frac{F(t)\int_0^l p(x)X_n(x)dx}{r\int_0^l X_n^2(x)dx} \tag{2.17}$$

In this paper, the focus is on the influence of construction materials on the theoretical value of the impact factor. Hence, a relatively simple case of a constant force F moving across the span of a beam at constant velocity v will be used.

From Eq. (2.14), the shape function has the form

$$X_n(x) = \sin(\frac{npx}{l})$$

Hence, the right-hand side of Eqs. (2.16) and (2.17) is replaced by

$$\frac{F\int_0^l p(x)\sin(\frac{npx}{l})dx}{rl/2}$$

where x is the distance from the end of the span to the force. Assume x is a function of time and is equal to vt, where t is measured from the instant at which the force entered the span. After substitution of x=vt, and p(x)=δ (x=vt) (δ function at x=vt, which means that p(x)=1 when x=0 and x=l, p(x)=0, otherwise), Eqs. (2.16) and (2.17) become

$$T_n''(t) + w_n^2 T_n(t) = \frac{2F}{rl}\sin(\frac{npvt}{l}) \tag{2.18}$$

$$T_n''(t) + 2x_n w_n T_n'(t) + w_n^2 T_n(t) = \frac{2F}{rl}\sin(\frac{npvt}{l}) \tag{2.19}$$

After imposing the initial conditions, y(x,0)=0 and y'(x,0)=0, the solution of Eq. (2.18) is

$$T_n(t) = \frac{2F}{rl}\frac{1}{w_n^2 - \Omega_n^2}(\sin \Omega_n t - \frac{\Omega_n}{w_n}\sin w_n t)$$

where $\Omega_n = npv/l$. Since $y(x,t) = \sum_{n=1}^{\infty} X_n(x)T_n(t)$, we obtain the total solution for the deflection

$$y_n(x,t) = \frac{2F}{rl}\sum_{n=1}^{\infty}\frac{1}{w_n^2 - \Omega_n^2}(\sin \Omega_n t - \frac{\Omega_n}{w_n}\sin w_n t)\sin(\frac{npx}{l})$$

If we assume viscous damping in each mode where where $g_n / w_n = x_n$ is the fraction of critical damping in the n-th mode, the solution then becomes

$$y_n(x,t) = \frac{2F}{rl}\sum_{n=1}^{\infty}\frac{\sin(npx/l)}{(w_n^2 - \Omega_n^2)^2 + 4(g_n\Omega_n)^2}\{(w_n^2 - \Omega_n^2)\sin \Omega_n t - 2g_n\Omega_n \cos \Omega_n t + e^{-g_n t}[2g_n\Omega_n \cos w_n t + \frac{\Omega_n}{w_n}(2g_n^2 + \Omega_n^2 - w_n^2)\sin w_n t]\} \quad (2.20)$$

which will be used as the governing equation of the system model in this research.

Numerical Examples

To evaluate the influence of construction materials on impact factors, three examples of bridges by reinforced concrete, steel, and timber will be taken based on the information by Barker and Puckett [15]. To get similar foundational characteristic for the bridges, three other examples with unique natural frequencies will be shown. The dynamic deflection is calculated by the governing Eq. (2.20). And the static deflection is based on the following formula,

$$y_{sta} = \frac{F(l - vt)l/2}{6lEI}[l^2 - (l - vt)^2 - (\frac{l}{2})^2] \qquad l/v \le t \le l/(2v)$$

$$y_{sta} = \frac{F(l - vt)l/2}{6lEI}[l^2 - (l - vt)^2 - (\frac{l}{2})^2] + \frac{F(l/2 - vt)^3}{6EI} \qquad 0 \le t \le l/(2v)$$

where

F: is the vehicle loading

l: is the span length of the bridge beam

v: is the velocity of the vehicle, and
t: is the time

Definition 8 of the impact factor using the static instead of the median displacement will be used in the examples because definition 8 is used in the AASHTO code and the bridge examples are designed based on the AASHTO code. For this case the impact factor is

$$IM=\frac{d_{dyn}-d_{stat}}{d_{stat}}$$

where

d_{stat} = maximum static deflection

d_{dyn} = maximum dynamic deflection

Calculations were performed using symbolic math in Maple and with Excel to process and plot the results. The dynamic impact factors at mid-span are presented in Figs. 2.3-2.4. Figure 2.3 corresponds to calculations obtained using examples 1-3 and Figure 2.4 corresponds to calculations obtained for examples 4-6. The ratio analysis of the impact factor is discussed in a following section.

A constant vehicle loading (F=100KN) with a constant velocity (v=30mile/hr, 13.41m/sec) will be assumed. An equivalent damping equal to 0.02 of critical damping (damping ratio x =0.02) also will be presumed for all the examples. The examples will be calculated from information on bridges as follows:

Example 1

A reinforced *concrete* T-beam bridge was designed for a 13.42m wide roadway and three-spans of 10.67m-12.8m-10.67m with a skew of 30 degrees. The first span of 10.67m evaluates the impact factor. The area of the T-beam (A) is 0.65475 m². The moment of inertia of the beam cross section (I) is

0.5315 m^4 . The Young's modulus (E) is 2.629e+10 Pa. The mass density is 2400 kg/m³. f'_c =30MPa, f_y =400Mpa. The impact factor, after calculation, is 0.033.

Example 2

A simple span non-composite rolled *steel* beam bridge with 10.5m span is designed. Roadway width is 13.42m curb to curb. Use f'_c =30MPa, and M270 Gr345 steel. The mass per length of the beam (r) is 134 kg/m. The moment of inertia and the Young's modulus are 1.5e-3m^4 and 1e+11 Pa, respectively. The impact factor of this example is 0.025.

Example 3

A *glulam* beam superstructure to span a 10.668m (35ft) center to center of bearing is designed. It carries two traffic lanes and has a roadway width of 7.3m (24ft). The mass per length of the beam (r) is 193.68 kg/m. The moment of inertia is 0.0108 m^4 , and the Young's modulus is 1.03e+10 Pa. The impact factor is 0.025 percent.

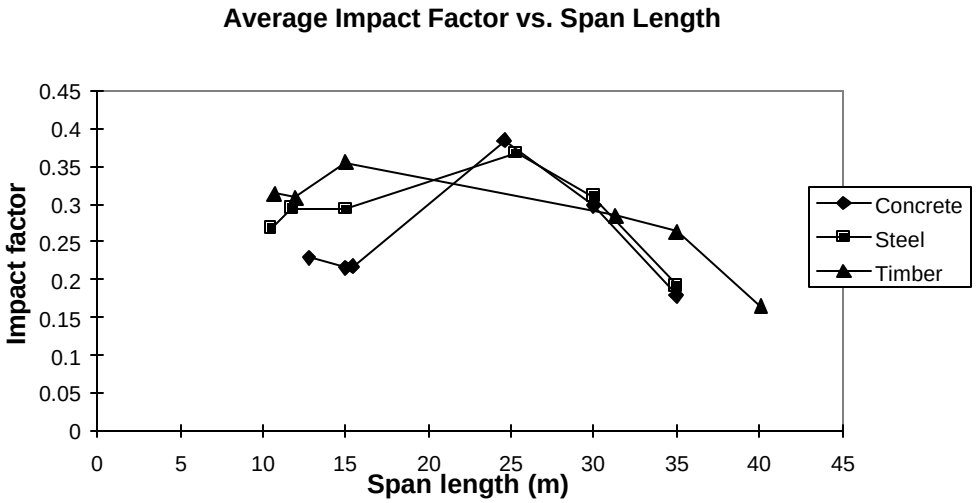

Figure 2.3: Average Impact Factor versus Span Length for Three Materials (Examples 1-3)

Now we set the natural frequencies of three bridges to be equal to 2n²p ² (HZ), and E, I, r remain unchanged. The next three examples, with equivalent natural frequencies will be a more accurate

method to evaluate the effect of different materials on impact factors. Because natural frequency is one of the basic characteristics of a structure, the comparison of bridge impact factors could be made on a similar basis, if they have the same natural frequency. The basic description of the systems for examples 4-6 are similar to those of example 1-3. The primary change is on the span lengths, which are 21.71m, 23m, and 19.46m for example 4 (*reinforced concrete*), 5 (*steel*), and 6 (*wood*), respectively. The impact factor is 0.069 for example 4, 0.071 for example 5, and 0.038 for example 6.

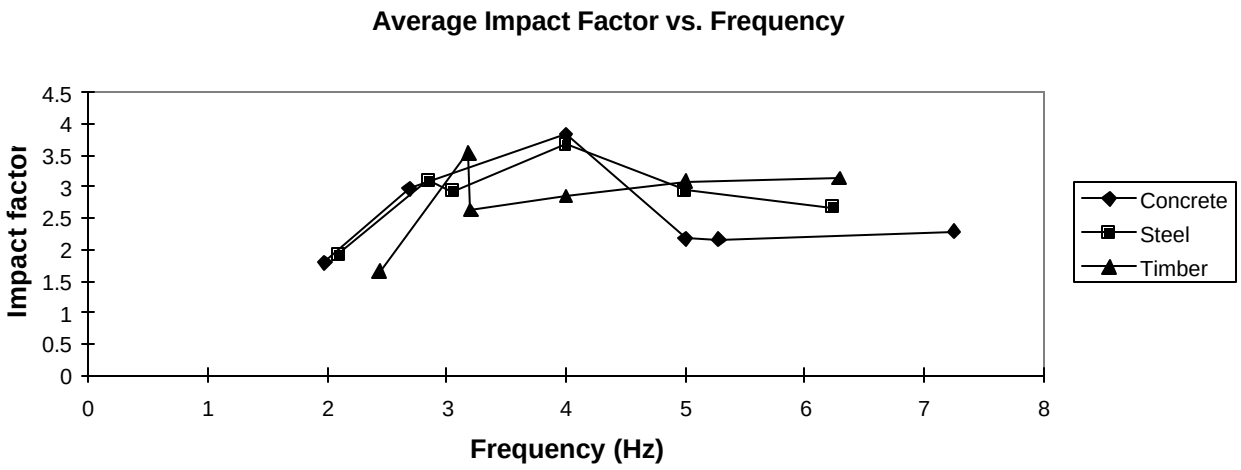

Figure 2.4: Average Impact Factor versus Frequency for Three Materials (Examples 4-6)

3. DISCUSSION AND RECOMENDATION

Discussion

From the numerical examples, the ratio of impact factors for reinforced concrete bridges, steel bridges, and wooden bridges may be obtained. Table 3.1 shows the ratios from examples 1-3, and Table 3.2 contains the ratios from examples 4-6. For cases 4-6 the bridge length is corrected so that the natural frequencies are the same.

Table 3.1: Ratio of impact factor of bridges built of three materials normalized to concrete design (each bridge design has different natural frequencies)

	Concrete bridge as one
Concrete bridge	1
Steel bridge	0.750751
Timber bridge	0.738739

Table 3.2: Ratio of impact factor of bridges built of three materials normalized to concrete design (bridge design altered to equivalent natural frequencies in all cases)

	Concrete bridge as one
Concrete bridge	1
Steel bridge	1.030479
Timber bridge	0.557329

Since equal natural frequencies provide a similar basis for comparison of the impact factor, the primary focus is on results shown in Table 3.2. From Table 3.2, we see that the impact factors for the reinforced concrete bridge and the steel bridge are close. The impact factor of the wooden bridge is about 45 percent less than the impact factor for concrete and steel bridges.

If we analyze the same six example bridges using several bridge design codes from different countries, the following results are obtained. Table 3.3 shows the impact factors, which are calculated for examples 1-6 according to international bridge design codes. The ratios of impact factors as shown for the calculated results for examples 1-3 and examples 4-6 are shown in Table 3.4 and Table 3.5, respectively. Note that it has been assumed that the structures designed are not in fatigue and fracture limit state. Also

because of the limited specifications for timber, the impact factor for wooden bridges are not shown for the Taiwanese code and the Eurocode.

Table 3.3: Impact factor according to international bridge design codes

	Example 1	Example 2	Example 3	example 4	Example 5	Example 6
AASHTO	0.33	0.33	0.165	0.33	0.33	0.165
OHBDC	0.3	0.3	0.21	0.3	0.3	0.21
Taiwan	0.3	0.3	----	0.2548	0.2494	----
Eurocode	1.43	1.44	----	1.21	1.2	----

Table 3.4: Ratio of impact factor (from examples 1-3)

	Concrete	Steel	wood
AASHTO	1	1	0.5
OHBDC	1	1	0.7
Taiwan	1	1	----
Eurocode	1	1	----

Table 3.5: Ratio of impact factor (from examples 4-6)

	Concrete	Steel	Wood
AASHTO	1	1	0.5
OHBDC	1	1	0.7
Taiwan	1	0.98	----
Eurocode	1	0.99	----

It is clear that any difference in the impact factor between concrete and steel bridges is small, no matter which code is applied. Consequently, it is useful to compare the ratio of the impact factor for examples 4-6 obtained from calculations based on the governing equation (2.20) with those from international codes (Table 3.6).

Table 3.6: Comparison of ratio of impact factor (from examples 4-6)

	Concrete	Steel	Wood
Eq. (2.20)	1	1.03	0.56
AASHTO	1	1	0.5
OHBDC	1	1	0.7
Taiwan	1	0.98	----
Eurocode	1	0.99	----

From Table 3.6, it is evident that there is a significant degree of divergence for the ratios of timber bridges. It appears from this work that the AASHTO code underestimates the impact factor of timber bridges, while the OHBDC uses a conservative estimate.

Although, based on concepts of Load Resistance Factor Design (LRFD), it is logical to extend the load factor to create an impact factor, the same percentage for impact factor results. Hence, one conclusion can be made from the simple system model used in this research; the impact factors for reinforced concrete and steel bridges are close, and given other types of uncertainty may be taken as identical. The impact factor for timber bridges appears to be about 45 percent below that of concrete or steel bridges. This impact factor is higher than the design factor used in the AASHTO code. However, more effort is required to verify the quality of this observation.

Recommendation

The following are recommendations for further study of influence of materials on bridge impact factors.

A simple model is used in this paper. However, many random variables exist in the interaction of moving vehicles and bridge systems. A more accurate system model is essential for a complete understanding of impact factors.

A large difference in research is evident between composite and non-composite materials. Construction methods also influence the material properties. Therefore, it is necessary to investigate the sensitivity of models to different properties which result from construction of bridges with different designs.

Constant, single-point, loading is used in this paper, however multi-point loading should be used to model multi-axle vehicle loading in future studies.

Multi-span bridge systems should be considered in future research.

The interaction of the suspension system of vehicle loading to the roadway roughness is a complex and important parameter in models of bridge dynamics. This extension is to include the suspension system of the vehicle loading has been shown to be important in predicting dynamic loading.

The dynamic impact factor is defined based on the ratio of dynamic deflection to static deflection. The stress rather than the deflection of the bridge is of primary importance. The relationship between the impact factor and resultant dynamic stress should be considered in future research.

REFERENCES

1. LRFD (Load and Resistance Factor Design) Bridge Design Specifications, AASHTO (American Association of State Highway and Transportation Officials), Washington D. C., 1994.

2. Eui-Seung Hwang and Andrzej S. Nowak, "Dynamic Analysis of Girder Bridges," 1989, Transportation Research Record 1223, pp 85-92, National Research Council, Washington D. C.

3. B. Bakht and S. G. Pinjarkar, "Dynamic Testing of Highway Bridges- A Review," 1989, Transportation Research Record 1223, pp 93-100, National Research Council, Washington D. C.

4. A. H. Fuller, A. R. Eitzen, and E. F. Kelly, "Impact on Highway Bridges," Transactions, ASCE, vol. 95, 1931, pp 1089-1117.

5. R. Cantieni, "Dynamic Load Tests on Highway Bridges in Switzerland : 60 years experience of EMPA," Report 271, Swiss Federal Laboratories for Materials and Testing Research, Dubendorf, 1983.

6. B. Bakht, "Soil-Steel Structure Response to Live Loads," Journal of the Geotechnical Engineering Division, ASCE, vol. 107, No. GT6, 1981, pp 779-798.

7. J. R. Billing, " Dynamic Loading and Testing of Bridges in Ontario," Proc., International Conference on Short and Medium span Bridges, Toronto, Canada, vol. I, 1982, pp125-139.

8. Ontario Highway Bridge Design Code, Ontario, Ministry of Transportation, Quality and Standards Divisions, Canada, 1983.

9. Paultre, P., U. Challal, and J. Proulx, "Bridge Dynamics and Dynamic Amplification Factors- A Review of Analytical and Experimental Findings," 1992, Canadian Journal of Civil Engineering, vol. 19, pp 260-278.

10. Ontario Highway Bridge Design Code, Ontario, Ministry of Transportation, Quality and Standards Divisions, Canada, 1991.

11. Highway Bridge Design Code, Ministry of Transportation, Taiwan, 1987.

12. Eurocode, Committee of European Normalization (CEN), 1995.

13. AASHTO Bridge Design Specifications, Washington D. C., 1989.

14. Introduction to Structural Dynamics, John M. Biggs, McGraw-Hill, Inc. 1964.

15. Design of Highway Bridges, Richard M. Barker and Jay A. Puckett, John Willey & Sons, Inc. 1997.